Title:

Alterations in photosynthesis and energy reserves in *Galdieria sulphuraria* during corn stover hydrolysate supplementation

Author names and affiliations:

Khadijeh Mozaffari [a], Mark Seger [b], Barry Dungan [a], David T. Hanson [c], Peter J. Lammers [b], F. Omar Holguin [a*]

[a] Department of Plant and Environmental Sciences, New Mexico State University, Las Cruces, NM 88003, USA.

[b] AzCATI, School of Sustainable Engineering and the Built Environment, Arizona State University, Mesa, AZ 85212, USA.

[c] Department of Biology, The University of New Mexico, Albuquerque, NM 87131-0001, USA.

E-mail address of co-authors:

Khadijeh mozaffari: mozafari@nmsu.edu; Mark Seger: mark.seger@asu.edu; Barry Dungan: bdungan@nmsu.edu; David T. Hanson: dthanson@unm.edu; Peter J. Lammers: Peter.Lammers@asu.edu;

[*] Correspondence author. Tel.: +1 575 646 5913; Fax: +1 575 646 6041.
E-mail: frholgui@nmsu.edu (F.Omar Holguin)

Abstract

The carbon allocation and alterations in the photosynthetic apparatus of the red microalga, G*aldieria sulphuraria* CCMEE 5587.1 were investigated under photoautotrophic, mixotrophic and heterotrophic conditions in this paper. Photosynthetic O_2 evolution values and chlorophyll *a* content decreased during one week of cultivation in both hetero- and mixotrophic cultivations. A 2.1-fold and 2.6-fold reduction was observed in phycocyanin content under mixo- and heterotrophic conditions, respectively. TEM microscopy confirmed that mixotrophic conditions favor carbon allocation toward starch biosynthesis along with an increase in the size of chloroplasts. In contrast, carbon is allocated toward lipid production under heterotrophic cultivation with apparent smaller multi-lobed chloroplasts. These results increase our understanding of the roles of photosynthesis and external carbon sources on bioenergy products from *Galdieria*.

Keywords

Galdieria sulphuraria; Corn stover hydrolysate (CSH); Fatty acids; β-glucan; Ultrastructure

1. Introduction

During photoautotrophic growth, microalgae utilize light and inorganic nutrients to produce biomass rich in high-value compounds. These molecules vary in chemical class such as lipids, proteins, pigments and long-chain polyunsaturated fatty acids (Graziani et al., 2013; Markou & Nerantzis, 2013). Microalgae are promising feedstocks because of their high

biomass productivity and their use for biofuel, food, feed and other important bioproducts (particularly under stress conditions) (Khan et al., 2018).

Mixotrophic algal metabolism resulting from utilization of organic carbon via respiration and CO_2 via photosynthesis can substantially increase algal biomass productivity and provide ecosystem services (Henkanatte-Gedera et al., 2017). Poly-extremophilic red microalgae in the genus *Galdieria* provide a particularly promising example because their tolerance to low pH values (0.5-5.0), elevated temperatures (35-56°C), brackish water and toxic metals provide strong selection against most potential contaminating heterotrophic microorganisms (Reeb & Bhattacharya, 2010). Because of the adaptation to extreme growth conditions, *Galdieria* spp. are useful organisms for bioenergetics studies using highly accessible carbon substrates. In fact *G. sulphuraria* can utilize over 27 different carbohydrates making it the most versatile mixo-/heterotrophic microalgae known to date (Gross et al., 1998; Gross & Schnarrenberger, 1995; Sloth et al., 2006). Under mixotrophic cultivation, different organic carbons such as glucose, glycerol, and sucrose are coupled with CO_2 utilization to combine the power of both photoautotrophic and heterotrophic growth (Dragone et al., 2010). As previously demonstrated, *G. sulphuraria* 074G reached the culture density of 110 g L^{-1} when grown on glucose (Graverholt & Eriksen, 2007). Moreover, the same strain had a higher yield (up to 166 g L^{-1}) when sugar beet molasses was utilized in heterotrophic and mixotrophic experiments (Schmidt et al., 2005). Others have also shown that *G. sulphuraria* exhibits high biomass productivity when cultured under heterotrophic conditions (Graverholt & Eriksen, 2007; Sakurai et al., 2016).

Nevertheless, photosynthetic activity is known to be markedly affected in heterotrophically grown *Galdieria sulphuraria* 107.79 using lactose as an organic carbon source by losing their photosynthetic apparatus (Tischendorf et al., 2007), glucose addition to strain *Galdieria sulphuraria* 074G behaves similarly (Oesterhelt et al., 2007). Heterotrophically grown *Galdieria sulphuraria* Soos strain lost all its pigments with reduced plastids using a wide range of organic substrates (Gross & Schnarrenberger, 1995). Here we examine *Galdieria sulphuraria* CCMEE 5587.1 (hereafter *G. sulphuraria* 5587.1) mixotrophic metabolism of cellulosic sugars, mainly glucose and xylose, derived from chemical degradation of corn stover yielding a low-cost corn stover hydrolysate (CSH). CSH is a renewable and environmentally sustainable alternative for mixotrophic metabolism due to its high concentration of fermentable sugars (Jang et al., 2012; Lau & Dale, 2009). The aim was to study carbon allocation and chloroplast ultra-structure changes using low-cost CSH substrates in *G. sulphuraria* 5587.1 by evaluating carbon distribution among storage molecules under photo-, mixo-, and heterotrophic conditions. In this study we present alterations in parameters of photosynthetic activity of CSH-supplemented cells such as chlorophyll content, phycocyanin, and O_2 evolution values. Additionally, we present a hypothesis for carbon allocation during CSH-supplemented mixotrophic and heterotrophic metabolism.

2. Materials and methods

2.1. Algal strain and culture conditions

Galdieria sulphuraria strain CCMEE 5587.1 was obtained from R. Castenholz (University of Oregon) (Toplin et al., 2008). Cultures were grown on new modified Cyanidium media

(500 mL) (Gross & Schnarrenberger, 1995) at pH 2.5 in 1L baffle flasks with two ports: one for sparging CO_2 enriched air and the second for sampling. Cultures were cultivated under photoautotrophic, mixotrophic and heterotrophic conditions with 12hrs light/12hrs dark cycles, 2% CO_2, and temperature varying between 35˚C (lights off) and 45˚C (lights on) at an incident light intensity of 150 µmol photons m^{-2} s^{-1}. The heterotrophic cultures were wrapped in aluminum foil to exclude light and incubated together with the other treatments to maintain the same temperature regime. Three biological replicates for each culture condition were performed. The growth medium contained 25mM hexose equivalent CSH as the organic carbon source. CSH was provided by the National Renewable Energy Laboratory (NREL) as a single stock which contained sugars in the following concentrations: glucose (200.16 g L^{-1}), xylose (110.85 g L^{-1}), arabinose (15.87 g L^{-1}), galactose (15.38 g L^{-1}) and cellobiose (8.8 g L^{-1}).

Heterotrophic, fed-batch fermentation was performed using a New Brunswick Bioflo IV 20L (15L working volume) bioreactor equipped with dissolved oxygen, pH, temperature, and antifoam control. The culture was started in Cyanidium media (CM), (Selvaratnam et al., 2015) twice the specified nitrogen and phosphorus components and 50 g L^{-1} glucose. The reactor was continuously agitated at ~500 rpm with two Rushton turbines coupled with 2.5 L min^{-1} air sparging. Temperature was maintained at 40˚C and pH kept between 1.5 and 2.5 using 3N KOH, respectively. Fed batch growth was conducted via manual additions of modified CM growth media in response to increases in dissolved oxygen. The modified, concentrated CM medium solutions for fermenter use contained 3-fold higher concentrations of all CM components except the following: 42-fold higher ammonium sulfate, 50-fold higher $FeCl_3$ plus 500 g L^{-1} glucose. When the culture volume reached 15 L

supplemental nutrient additions followed the removal of equal volumes of culture to maintain the total volume at 15 L (Schmidt et al., 2005). These occurred 1-3 times daily and volumes ranged from 0.5-1.0 L. Substrate yields were calculated for the 5 days of constant-volume growth based on the sum of all the biomass fractions produced in grams ash-free dry weight (AFDW)/sum of glucose added.

2.2. Optical density and specific growth rate measurement

Optical density (OD) was measured daily using a UV/Vis Spectrophotometer (DU 530, Beckman Coulter, US) at 750 nm during the middle of the light cycle under all growth conditions. Samples for analysis were taken at inoculation, log phase, and stationary phase. The following equations were used to calculate the (1) estimated biomass density AFDW (Selvaratnam et al., 2014), (2) maximum specific growth rate and (3) biomass yield coefficient (Widdel, 2007):

(1) $AFDW = 0.54 \times OD750 + 0.023$

(2) $\mu = (\ln\ OD_2 - \ln OD_1)/(t_2 - t_1)$

(3) $Y_{x/s} = (X_t - X_0) / (S_t - S_0)$

2.2. Nutrient assays

Samples were centrifuged at 10,000 rpm and the supernatant was used for daily nutrient uptake analysis and media substrate analysis. The resulting cell pellets were saved for the chlorophyll analysis. Nutrient uptake was quantified for ammonium and phosphate with microplate assay protocol as described by Hernández-López & Vargas-Albores (Hernández-López & Vargas-Albores, 2003). For the ammonium sulfate analysis, 250 µL of the supernatant was used in the reaction. The solution containing hypochlorite reacts with the

ammonia which is formed in the solution giving the blue color. The absorbance was recorded after 60 min incubation at room temperature at 655 nm. For the potassium phosphate analysis, supernatant was diluted (500 fold) in distilled water, then 250 µL of dilution was used for the analysis in the reaction mixture. The ammonium molybdate in the solution containing ascorbic acid reacts with phosphate resulting in a blue color. After a 10 min incubation period at room temperature the absorbance was read at 655 nm (Hernández-López & Vargas-Albores, 2003). Standards were prepared as serial dilutions from 1.5 mM KH_2PO_4 and $(NH_4)_2SO_4$ stock solutions, and used to generate standard curves.

2.3. Media substrate analysis

Concentrations of saccharides of CSH in the growth medium was analyzed using a gas chromatography time of flight mass spectrometry (GCTOF-MS) composed of a 7890A GC System (Agilent Technologies, US) and a Leco Pegasus HT High Throughput TOF-MS (Leco, US). The supernatant was derivatized as previously described by Lee and Fiehn (2008) and analyzed within 24hrs (Lee & Fiehn, 2008). Briefly, 200µL of supernatant dried in a speed vac and 2µL of fatty acid methyl ester mix (Sigma Aldrich, Product No.49453-U) was added as an internal retention index to the dried samples along with 10µL of a solution of 20 mg/mL of methoxyamine hydrochloride (Sigma-Aldrich, St. Louis, MO, US) in pyridine (Sigma-Aldrich, St. Louis, MO, US) and shaken at 30°C for 90 min. Then 45 µL of MSTFA 0.1%TMCS (Pierce, Rockford, IL) was added to the samples and shaken at 37°C for 30 min. Serial dilutions of carbohydrate standards of glucose, xylose, arabinose, cellobiose and galactose, (Sigma-Aldrich, St. Louis, MO, US) were generated for the quantification of saccharides in the samples. The spectral data from each carbohydrate were

processed after data acquisition with their unique characteristic ions. These data were search against the Fiehn metabolomics library. Peak integration and alignment was performed in MET-IDEA V2.08 (Noble Foundation, Oklahoma, US) for both the samples and standard carbohydrate mix.

2.4. Chlorophyll *a* & Phycocyanin measurements

Chlorophyll *a* (Chl) was extracted from the pellets saved from nutrient analysis using 80% (v/v) acetone. Chl content in the extracts was measured spectrophotometrically (DU 530, Beckman Coulter, US) and further quantified using coefficients as described previously by Ritchie (Ritchie, 2006). Phycocyanin (PC) measurements were made from cell pellets, samples were centrifuged at 4,000×g for 10 min and subsequently washed with distilled water twice and frozen at -20°C for analysis. The cells were lyophilized, resuspended in 0.10 M Na_2HPO_4/NaH_2PO_4 (MilliporeSigma, St. Louis, MO, US) pH 7.0 and disrupted with 0.1 mm silica beads in a homogenizer (Precellys 24, Bertin Technologies) at 6,500 rpm (3x 30 seconds) followed by centrifugation at 16,000×g for 60 min. The PC concentration was determined at 618 nm from in vivo absorbance spectra as described by Kursar and Alberte (Kursar & Alberte, 1983).

2.5. Oxygen evolution

For the direct O_2 evolution measurement, the data were collected at the 1st (log phase), 4th (exponential phase) and 7th day (stationary phase) from each conditions (n =3) and measured using a Firesting O_2 meter (Pyro Science, US) with respiration vials. For the

gross O_2 evolution, the net O_2 evolution was measured for 5 min at 150 µmol photons m^{-2} s^{-1} followed by the O_2 consumption immediately in the dark for 1 min.

2.6. Electron microscopy

Aliquots of cultured cells in both exponential and stationary phases were chemically-fixed by addition of glutaraldehyde (Electron Microscopy Sciences, Hatfield, PA) with rapid mixing to a concentration of 2.5%, and the cells were harvested by centrifugation at 3,000×g. The resulting cell pellets were embedded in 4% low-melt agarose (Sigma-Aldrich, St. Louis, MO, US) and subsequently processed by post-fixation in 2% osmium tetroxide (Electron Microscopy Sciences, Hatfield PA) solution buffered with 0.1 M imidazole-HCl, pH 7.2. The cells were washed in de-ionized water, dehydrated with a graded series of ethanol solutions and embedded in Spurr's epoxy resin (Low viscosity embedding kit, Electron Microscopy Sciences, Hatfield, PA) before oven curing at 60°C for 48hrs. Digital images of selected cell profiles were captured with a model XR611 mid-mount digital camera (Advanced Microscopy Techniques, Woburn, MA).

2.7. Fatty acid methyl ester determination (FAME)

For the analysis of total fatty acid content, the cells were harvested by centrifugation and then lyophilized. Approximately 15 mg of dry biomass were added in vials, and extracted using 200 µL of chloroform:methanol (2:1 v/v). Fatty acids were esterified using 300 µL 0.6M hydrochloric acid:methanol (Van Wychen & Laurens, 2013) and placed on dry heating blocks at 85°C for an hour. Then 0.5 mL hexane was added to each of the vials for extraction and subsequently analyzed by Varian 3900 GC FID (Varian, US). FAMEs were

separated chromatographically using a DB-23 capillary column (60m × 0.25 mm × 0.25 μm). The injector temperature was kept at 250°C with the sample injection of 2 μL. The oven temperature setting was as followed; 100°C for 1 min, ramping at 25°C min^{-1} up to 200°C, held at 200°C for 1 min, from 200°C to 250°C at the rate of 3°C min^{-1} with a hold of 7 min. Hexane with an internal standard solution (C23:0, methyl tricosonate, at 50 μg mL^{-1}) and standard curve from a serial diluted Supelco FAMEs mix (Sigma-Aldrich, St. Louis, MO, US) was used to quantify peaks in samples.

2.8. Starch and β-glucan analysis

Approximately 20 mg of lyophilized tissue was used for analysis of total starch content. Glucose was first removed from samples with 80% (v/v) ethanol, the residual starch was hydrolyzed to glucose following incubation with α-amylase and amyloglucosidase at 50°C for 30 min (Total starch assay, Megazyme, Wicklow, IRELAND). For the β-glucan analysis, the (1,3)/(1,6)-β-glucans were measured with Glucazyme enzyme incubation (Enzymatic yeast Beta-glucan assay, Megazyme Wicklow, IRELAND). Free glucose was quantified spectrophotometrically at 510 nm as described in the Megazyme protocol.

2.9. Statistical analysis and experimental replication

All statistical analyses was performed in SAS version 9.4 software (SAS Institute, Cary, NC, USA). Three experimental conditions were performed on three plates to represent three biological replicates of each treatment. The effects of growth conditions on starch, PC and FAME profile in a 7-day period were analyzed using ANOVA with post hoc (LSD test) analysis. The letters A and B were used only for the graphs with statistical significance between variables ($p < 0.05$). The graphs with no letters were not statistically significant.

3. Results and discussion

3.1. Specific growth rate and biomass yield

The biomass productivity was significantly higher in the mixotrophic (M) and heterotrophic (H) cultures from exponential to stationary phase when compared to the photoautotrophic (A) cultures (Fig. 1A). Cells rapidly increased to 1.23 ± 0.06 and 1.29 ± 0.05 at OD750 after day 4 in in their exponential phase in hetero- and mixotrophic cultures respectively, while it reached 0.81 ± 0.07 under photoautotrophic conditions. Cultures grown mixotrophically performed similarly to those grown heterotrophically (Fig.1A). The cells maximum specific growth rate (μ_{max}) under mixo- and heterotrophic conditions were 0.228 ± 0.04 and 0.23 ± 0.03 respectively, and only slightly higher than photoautotrophic cultivation (μ=0.158 ± 0.07). However, Lammers et al. (2018, unpublished data) showed a 2-3 fold increase in mixo- and heterotrophic productivity relative to photoautotrophic productivity. The difference is likely due to lower oxygen availability in this study. Increased growth rates of acidophilic *G. sulphuraria* and *G. partita* under mixotrophic growth condition were previously reported (Oesterhelt et al., 2007; Stadnichuk et al., 1998). One possible explanation for our lower productivity is the combined effects of the limitations on oxygen mass transfer and light in 1L baffle flasks used in our experiment.

3.2. *G. sulphuraria* nutrient uptake

To test whether or not nutrition limitation is playing role in the biomass growth, nutrient uptake was measured using ammonium and phosphate. Ammonium levels in the culture decreased during the 7-day growth period in all growth conditions. Total ammonium

content decreased by 5.6%, 38.2% and 38.5% after day7 under photoautotrophic, mixotrophic and heterotrophic conditions respectively (Fig. 1B). Moreover, total phosphate concentration was reduced under all treatments with the highest uptake under the heterotrophic condition with over 40% and 50% reduction in mixo- and heterotrophic cultures. Despite the higher biomass production, there was a minor reduction in ammonium uptake with hetero- and mixotrophic conditions, as other researchers also showed the similar results with nitrogen availability and limitation (Schmidt et al., 2005; Sloth et al., 2006). Higher biomass growth obtained under heterotrophic cultivation might be the reason we observe more ammonium uptake rates under such condition. Moreover, increased phosphate uptake was noticed in the cultures grown in heterotrophic than mixotrophic condition on the last day of the 7-day growth period. Our data suggested higher phosphate uptake than nitrogen in *Galdieria sulphuraria* that is supported by the phosphate to nitrogen ratios which decreased over 7-day cultivation conditions mixo- and heterotrophically. These results showed that there was no significant reduction in ammonium concentration in both mixo- and heterotrophic cultures. Moreover, photoautotrophic cultures were not ammonium-limited during the stationary phase of growth.

3.4. Corn stover hydrolysate uptake.

G. sulphuraria cultures were analyzed for CSH sugars (glucose, xylose, galactose, arabinose, and cellobiose) throughout the growth period. Substrate yields were 0.36 and 0.27 g-biomass g-sugar $^{-1}$ for the mixotrophic and heterotrophic cultivation respectively during the maximum growth period between day3 and 4 (Fig. 2A). These values are less

than previous reports in cultures grown on glucose and waste hydrolysates (Sakurai et al., 2016; Sloth et al., 2017). Previously, heterotrophic substrate yields of 0.42-0.52 have been reported for *G. sulphuraria* O74G grown in aerobic fermenters (Graverholt & Eriksen, 2007). Additionally, our previous research showed mixotrophic substrate yields of 0.6-1.0 in flat-panel and tubular photobioreactors (Lammers et al., 2018, unpublished data) with *G. sulphuraria* 5587.1 using glucose, sucrose or the same batch of CSH used here. *G. sulphuraria* 5587.1 was grown in an aerobic fermenter, yielded a heterotrophic substrate yield of 0.43, thus eliminating genetic differences between *G. sulphuraria* O74G and 5587.1 as the cause of the lower than expected response to sugars.

We conclude the deviations from previous reported substrate yields were likely caused by sub-optimal O_2 levels due to the combined effects of the long light path in Erlenmeyer flasks (11.4 cm at bottom) and limitations on mass transfer of oxygen in half-full, baffled shake flasks.

The *Galdieria* cells metabolized glucose and xylose completely by day 7 heterotrophically with glucose, and galactose being the most preferentially used saccharides (Fig. 2B). The concentration of cellobiose was lowest with respect to other saccharides in the CSH. Interestingly cells under heterotrophic cultivations used up cellobiose completely (Fig. 2B) while mixotrophic cells used only half of the cellobiose (Fig. 2C).

3.3. Chlorophyll, oxygen evolution & phycocyanin measurements

Photosynthetic O_2 evolution, evaluated by the direct measurement of photosystem II (PSII) activity, increased under photoautotrophic conditions compared to mixo- and heterotrophic

conditions (Fig. 3A). Heterotrophic cultures were deplete of O_2 by 24 hrs. Since there is no light, extra O_2 provided by PSII is not readily available in these cultures. While the cultures cultivated under mixotrophic conditions exhibited a significant drop in O_2 evolution, levels of O_2 stabilized in the cultures from day 4 (exponential phase) on. This indicates the O_2 production (PSII) is in equilibrium with O_2 consumption (respiration; sugar consumption). Chl content dropped in a similar rate when comparing the two treatments (Fig. 3B), while there is a stark difference in the drop in O_2 evolution rate with the heterotrophic cultures. The slower decline in the mixotrophic cultures suggest that they are still evolving O_2 and barely matching respiration (glucose metabolism). Without light in the heterotrophic cultures, PSII would be completely down-regulated. There is no light in the heterotopic conditions so photosynthesis is already down regulated. The decrease in O_2 evolution seen in the first day is essential for the cells taking up the available O_2 found in the culture/media. Finally, normalized O_2 evolution values (μmol O_2 [mg Chl]$^{-1}$ min^{-1}) also showed similar upward trends under photoautotrophic condition while it decreased rather slowly under mixotrophic condition relative to rapid reduction heterotrophically (Fig. 3C). These data together confirmed the reduced performance of photosynthesis under mixotrophic condition which has been previously described in other *G. sulphuraria* strains cultivated under mixotrophic conditions with glucose supplementation (Oesterhelt et al., 2007; Stadnichuk et al., 1998; Tischendorf et al., 2007). However, the comparison of gross O_2 evolution showed that the photosynthetic O_2 evolution does to some extent occur in cells under mixotrophic conditions later during the stationary phase of growth. However, in order to validate the idea of the net conversion from respiration to photosynthesis in

mixotrophic condition, it would be interesting to observe the O_2 evolution changes in post-stationary phase.

Growth, O_2 evolution and carbohydrates analysis illustrate the physiology of cellular carbohydrate uptake in mixotrophic and heterotrophic cultures. During the period of high growth, heterotrophic cells use the carbohydrates with an increase in growth and a decrease in gross O_2 evolution as expected. During the light periods of mixotrophic growth, algal cells demonstrate photosynthetic activity as evidenced by the slower drop in O_2 under the mixotrophic condition compared to the heterotrophic condition. The GC/MS analysis of the CSH and O_2 evolution data showed that as the sugar concentrations approached zero the respiration rate decreased which further showed less probability of respiration event in heterotrophic cultures. Photoautotrophic cultures exhibited higher O_2 evolution rate, which is suggestive of increase in photosynthetic activity (Fig. 3A).

Production of PC was investigated in all treatment conditions. The PC concentration decreased significantly from 7.5 mg g^{-1} DW under photoautotrophic cultivation to 3.5 mg g^{-1} DW and 2.84 mg g^{-1} DW under hetero- and mixotrophic conditions, respectively (Fig. 3D). PC content in the photoautotrophic cultures was significantly higher than the CSH supplemented cells in both exponential and stationary growth phases which further validates down-regulation in photosynthetic activity in such cells (Fig. 3D). Factors such as the limited carbon and nitrogen availability and also lower light intensity increase the PC synthesis in *G. sulphuraria* (Sloth et al., 2006). Although the nutrient and carbon limitation was not observed in both mixo- and heterotrophic cultures (exponential phase) in our study, PC concentration was equally low in both the culture conditions. Even though sugar

sources such as glucose increase the biomass and PC productivity (Eriksen, 2018; Sloth et al., 2006), it has been shown that sugar represses the PC content and synthesis in *Galdieria* (Oesterhelt et al., 2007; Stadnichuk et al., 2000). The reported higher PC content after complete depletion of sugar (Eriksen, 2008; Schmidt et al., 2005; Sloth et al., 2006) further highlights the important role of carbon limitation while nitrogen is still available and suggests a likely role for PC as a nitrogen storage compound in *Galdieria*. We found the CSH repression of light-induced PC synthesis effect in *G. sulpuraria* 5587.1. These results demonstrated the *G. sulphuraria* 5587.1 as a variant of a red alga that represses PC synthesis under the CSH regardless of nitrogen availability that is supported by significant reduction levels of PC under CSH supplementation. These data correspond to the previous studies on the negative effect of glucose on pigment biosynthesis in *G. sulphuraria* 074 G (Gross & Schnarrenberger, 1995). Therefore, the presence of CSH leads to the down-regulation of the photosynthetic O_2 evolution, as well as to reduced levels of PC content. PC content analysis after CSH depletion in the cultures in a post stationary phase will improve understanding of its role in *G. sulphuraria* 5587.1. The reduction in PC content in the presence of CSH most likely suggests the PC degradation as the cell's response to maintain cell viability until favorable growth conditions return.

3.5. Ultrastructure of *G. sulphuraria* cells

Images of thin sections contained evidence of many structures related to potential sites of carbon allocation as well as minor structural variations in the ultrastructure of chloroplasts within cell profiles. Cells in samples of auto- and mixotrophic cultures contained bigger chloroplasts with regular thylakoid membranes (Fig. 4A-D) whereas chloroplasts in cells

grown under heterotrophic conditions were smaller in size (Fig. 4E, 4F). In previous studies of *Galdieria*, the observed size of chloroplasts was smaller than heterotrophic conditions while under autotrophic conditions, a prominent chloroplast occupied most of the cell volume (Gross et al., 2002). Although in all the growth conditions studied, the chloroplast was pleomorphic or multilobular in mature and old-aged cells, usually we observed smaller lobed chloroplasts along with several vacuoles within larger cells (6-7μm) under heterotrophy. In the present study, cell sizes in heterotrophic and mixotrophic cultures were variable under CSH supplementation. Profiles of smaller cells contained starch and lipid structures while cells greater than 7μm (and groups of cells separated by cell walls) were dividing and displayed little or no evidence of organelles typically related to stored energy reserves (i.e., starch granules or lipid droplets).

Heterotrophically grown cells consistently contained numerous electron-dense circular profiles located between membranous lamellae chloroplasts, possibly representing lipid bodies (Fig. 4E, 4F) as opposed to larger circular electron-lucent areas or granules which could probably represent floridean starch accumulations under mixotrophic growing conditions (Fig 4C, 4D). In our study, these electron-dense circular bodies that are larger under heterotrophic condition than mixo- and photoautotrophic cultivations might be identified as plastoglobules (PG). PG are seen attached to thylakoids margins involved in lipid channeling (Bréhélin et al., 2007). Lipid remodeling in plants illustrated PG enlargement with thylakoid degradation as an adaptation to stress conditions (Rottet et al., 2015). PG are required for proper function of the thylakoid membrane and most of its components exist in green and red algae (Lohscheider & Bártulos, 2016). A research on

green algae *Dunaliella* concluded that the PG elevated under nitrogen limitation as a stress factor (Davidi et al., 2015). The presence of PG with electron dense aggregates in the stroma was also observed in *Galdieria* (Pinto et al., 2003). Thus it is possible that these lipophilic droplets represent PG in *Galdieria* under CSH supplementation. Because of the energy store profiles observed in our images, we concluded that the CSH supplementation favored starch production in mixotrophic condition while the heterotrophic nutritional conditions were more favorable toward lipid production.

3.6. Alterations in starch and Fatty acid methyl esters (FAME)

There are different types of starches such as glycogen-type and amylopectin-type (floridean starches) in Rhodophyta. The α-glucan starches in red algae proceed from UDP-glucose which is similar to ADP-glucose in glycogen synthesis pathway in prokaryotes (Viola et al., 2001). These starches are used as the primary source of energy storage and lipids as secondary storage compounds. They are significant elements of red algal cells, vital for cell growth, development and biodiesel production as well as a substrate for resistant polymer production (Martinez-Garcia et al., 2017; Shimonaga et al., 2008). These storage compounds can be overproduced using nutrient starvation, high salt and iron concentrations, and heterotrophic/mixotrophic culture conditions (Brányiková et al., 2011; Dragone et al., 2011; Liu et al., 2008; Martinez-Garcia et al., 2016; Sakurai et al., 2016; Takagi & Yoshida, 2006). Sulfur limitation caused starch-rich biomass in *Chlorella* and *Chlamydomonas* whereas nitrogen and phosphorus limitation increased higher starch content but their viability decreased over time (Brányiková et al., 2011; Zhang et al., 2002). Other researchers showed that the excess carbon is diverted into TAG and starch production under nitrogen starvation.

Nitrogen derived from amino acid catabolism was converted to intermediates and excess carbon diverted into starch mixotrophically and to storage lipid production heterotrophically (Scott et al., 2010). Lipid content in *Chlorella sorokiniana* reached to 51% under mixotrophic growth on glucose (Wan et al., 2011). Moreover, *Chlorella pyrenoidosa* produced significantly higher lipid productivity under mixotrophic cultivation using piggery wastewater (Wang et al., 2012). A previous report on *G. sulphuraria* SAG 108.79 showed higher glycogen production heterotrophically using the glycerol as the external carbon source (Martinez-Garcia et al., 2016). The red microalga, *Galdieria sulphuraria* 074W grown on various carbohydrate sources, produced higher starches mixotrophically whereas it produced higher lipids heterotrophically under glucose supplementation (Sakurai et al., 2016).

In our study, the amounts of α-glucan, β-glucan and FAME were analyzed during the exponential (Day 4) and stationary (Day7) phases (Fig. 5A-C). The starch granules increased significantly under the exponential phase of mixotrophic and heterotrophic conditions while it decreased during the stationary phase of the growth in all treatments with no significant differences between the treatments (Fig. 5A). The apparent decrease in starch during the stationary phase might be due to the cell's response during cellular division to favor the energy consumption (Vítová et al., 2011). Thus starch degradation during the stationary phase of the growth in all treatment condition is independent of light as also proposed by (Brányiková et al., 2011). The higher starch and lipid production, especially at the exponential phase, was further confirmed with our TEM microscopy (Fig. 4C-D). Moreover, we observed other storage carbohydrates which are found as a form of soluble dietary carbohydrate; β-

glucans. The β-glucans content increased at the stationary phase of mixotrophic condition, but there was no statistical difference between the treatments (Fig. 5B).

Our FAME results showed higher total FAME at the stationary phase of heterotrophic (5.06%) and autotrophic cultivations (5.45%) than mixotrophic cultures (3.55%) (Fig. 5C). The carbohydrate stored during the exponential phase in heterotrophy gets channeled toward the lipid production with more nutrient availability. The abundant availability of nutrients might have facilitated the less growth with higher lipid production in heterotrophic cultures at their exponential phase. Whereas, the apparent higher nutrient uptake, channeled the excess carbohydrate toward the higher starch production in mixotrophic cultivation (Fig. 5A-C). There was a significant reduction in lipid content under mixotrophic condition in the stationary phase compared to autotrophic and heterotrophic cultivations. C16:0 and C18:2 are the most dominant fatty acids present in fatty acid pool in all culture conditions while C18:3 are present in hetero- and mixotrophic cultivations (Fig. 5D-F). Overall, total fatty acid content was higher under heterotrophic cultivation relative to mixotrophic cultivation which is consistent with the previous research using glucose as the carbon source (Sakurai et al., 2016). Thus, mixo- and heterotrophically-grown cells resulted in higher biomass yield over the photoautotrophic samples during the 7-day period. Heterotrophic cells utilized the carbohydrates by day7, thus we concluded that CSH sugars primarily support energy production, cell division and favor lipid accumulation under heterotrophic condition. The increased biomass productivity under mixotrophic condition was characterized by higher growth and O_2 evolving capacity relative to heterotrophic condition. The slower reduction of the O_2 evolution rate in

mixotrophic cells is interpreted as simultaneous photosynthesis and respiration leading to increased production of intracellular O_2, NADPH, and ATP over heterotrophic cultures. The O_2 evolving capacity of cells grown mixotrophically decreased at a similar rate to that of Chl and PC reduction. Our results led us to conclude that CSH caused the photosynthetic down-regulation in *G. sulphuraria* 5587.1 under the experimental conditions here. In addition, CSH is stored as starches particularly during the exponential growth phase that can be metabolized later via pentose phosphate pathway in the light. Our hypothesis was that mixotrophic cells would use the power of both CSH and photosynthesis to produce significantly higher biomass and energy reserves than photoauto- and heterotrophic cells. Our results showed higher biomass yield during the exponential growth phase under mixotrophic cultivation. However, we did not observe significantly higher energy reserves in mixotrophic cultivation compared to heterotrophic cultivation. Under the conditions used here CSH uptake likely activates glucose catabolism and photosynthetic decline via catabolite repression of photosynthesis (Oesterhelt et al., 2007). Catabolite repression of photosynthesis has also been proposed in higher plants, where an excess supply of carbon can repress photosynthesis, and storage carbon reserves (Paul & Pellny, 2003).

4. Conclusions

Our results demonstrate that *G. sulphuraria* metabolizes CSH mono-saccharides to increase biomass productivity and carbon reserves. CSH supplementation resulted in a reduction of the photosynthetic pigments. Mixotrophic cells were able to maintain their O_2 evolving capacity to some extent while decreasing throughout the growth period. The fatty acid C18:3 concentrations increased in the cells grown heterotrophically at the stationary phase. Since

photosynthetic membranes contain significant levels of unsaturated fatty acids, low levels of unsaturation and higher saturation in mixo- and heterotrophically grown cells at the stationary phase might be in part associated with lipid remodeling in photosynthetic membrane.

Conflicts of Interest

The authors declare no conflict of interest. The funding agencies have no role in designing and conducting experiments, or in data analysis, in the writing of manuscript or in the decision to publish this article.

Acknowledgement

The authors would like to thank Dr. Peter Cooke for his skillful technical support and suggestions for EM microscopy and Sergei Shalygin for the graphical design. This research project was supported by the Department of Energy [award Project DE-EE0007562]; National Science Foundation [award number IIA-1301346] and the NMSU Agricultural Experiment Station.

Supplementary data

E-supplementary tables for the culture medium receipt for the experimental conditions, the phosphate to nitrogen ratio, Ash-free dry weight (AFDW), and the figures for the growth curve of 8-days cultures, TEM microscopy of heterotrophically grown mature cells can be found in online version of the paper.

References

Brányiková, I., Maršálková, B., Doucha, J., Brányik, T., Bišová, K., Zachleder, V., Vítová, M. 2011. Microalgae—novel highly efficient starch producers. Biotechnol Bioeng. **108**, 766–776. https://doi.org/10.1002/bit.23016

Bréhélin, C., Kessler, F., van Wijk, K.J. 2007. Plastoglobules: versatile lipoprotein particles in plastids. Trends Plant Sci. **12**, 260–266. https://doi.org/10.1016/j.tplants.2007.04.003

Davidi, L., Levin, Y., Ben-Dor, S., Pick, U. 2015. Proteome analysis of cytoplasmatic and plastidic β-carotene lipid droplets in Dunaliella bardawil. Plant Physiol. **167**, 60–79. https://doi.org/10.1104/pp.114.248450

Dragone, G., Fernandes, B.D., Abreu, A.P., Vicente, A.A., Teixeira, J.A. 2011. Nutrient limitation as a strategy for increasing starch accumulation in microalgae. Applied Energy, **88**, 3331–5. https://doi.org/10.1016/j.apenergy.2011.03.012

Dragone, G., Fernandes, B.D., Vicente, A.A., Teixeira, J.A. 2010. Third generation biofuels from microalgae. http://hdl.handle.net/1822/16807

Eriksen, N.T. 2018. Heterotrophic Production of Phycocyanin in Galdieria sulphuraria. in: *Extremophil*es: From Biology To Biotechnology, 2018, p. 87-101 CRC Press, pp. 87–102. 10.1201/9781315154695

Eriksen, N.T. 2008. Production of phycocyanin—a pigment with applications in biology, biotechnology, foods and medicine. Appl Microbiol Biotechnol. **80**, 1–14. https://doi.org/10.1007/s00253-008-1542-y

Graverholt, O.S., Eriksen, N.T. 2007. Heterotrophic high-cell-density fed-batch and continuous-flow cultures of Galdieria sulphuraria and production of phycocyanin. Appl Microbiol Biotechnol. **77**, 69–75. https://doi.org/10.1007/s00253-007-1150-2

Graziani, G., Schiavo, S., Nicolai, M.A., Buono, S., Fogliano, V., Pinto, G., Pollio, A. 2013. Microalgae as human food: chemical and nutritional characteristics of the thermo-acidophilic microalga Galdieria sulphuraria. Food Func. **4**, 144–152. 10.1039/C2FO30198A

Gross, W., Küver, J., Tischendorf, G., Bouchaala, N., Büsch, W. 1998. Cryptoendolithic growth of the red alga Galdieria sulphuraria in volcanic areas. Eur J Phycol. **33**, 25–31. https://doi.org/10.1080/09670269810001736503

Gross, W., Oesterhelt, C., Tischendorf, G., Lederer, F. 2002. Characterization of a non-thermophilic strain of the red algal genus Galdieria isolated from Soos (Czech Republic). Eur J Phycol. **37**, 477–483. https://doi.org/10.1017/S0967026202003773

Gross, W., Schnarrenberger, C. 1995. Heterotrophic growth of two strains of the acido-thermophilic red alga Galdieria sulphuraria. Plant Cell Physiol. **36**, 633–638. 10.1093/oxfordjournals.pcp.a078803

Henkanatte-Gedera, S.M., Selvaratnam, T., Karbakhshravari, M., Myint, M., Nirmalakhandan, N., Van Voorhies, W., Lammers, P.J. 2017. Removal of dissolved organic carbon and nutrients from urban wastewaters by Galdieria sulphuraria: Laboratory to field scale demonstration. Algal Res. **24**, 450–456. https://doi.org/10.1016/j.algal.2016.08.001

Hernández-López, J., Vargas-Albores, F. 2003. A microplate technique to quantify nutrients (NO2−, NO3−, NH4+ and PO43−) in seawater. Aquac. Res. **34**, 1201–1204. https://doi.org/10.1046/j.1365-2109.2003.00928.x

Jang, Y.-S., Malaviya, A., Cho, C., Lee, J., Lee, S.Y. 2012. Butanol production from renewable biomass by clostridia. Bioresour Technol. **123**, 653–663. 10.1016/j.biortech.2012.07.104

Khan, M.I., Shin, J.H., Kim, J.D. 2018. The promising future of microalgae: current status, challenges, and optimization of a sustainable and renewable industry for biofuels, feed, and other products. Microb Cell Fact. **17**, 36. 10.1186/s12934-018-0879-x.

Kursar, T.A., Alberte, R.S. 1983. Photosynthetic unit organization in a red alga: relationships between light-harvesting pigments and reaction centers. Plant Physiol. **72**, 409–414. 10.1104/pp.72.2.409

Lau, M.W., Dale, B.E. 2009. Cellulosic ethanol production from AFEX-treated corn stover using Saccharomyces cerevisiae 424A (LNH-ST). Proc. Natl. Acad. Sci. U.S.A. 1**06**, 1368–1373. 10.1073/pnas.0812364106

Lee, D.Y., Fiehn, O. 2008. High quality metabolomic data for Chlamydomonas reinhardtii. Plant methods. **4**, 7. https://doi.org/10.1186/1746-4811-4-7

Liu, Z.-Y., Wang, G.-C., Zhou, B.-C. 2008. Effect of iron on growth and lipid accumulation in Chlorella vulgaris. Bioresour Technol. **99**, 4717–4722. 10.1016/j.biortech.2007.09.073

Lohscheider, J.N., Bártulos, C.R. 2016. Plastoglobules in algae: a comprehensive comparative study of the presence of major structural and functional components in complex plastids. Mar Genomics, **28**, 127–136. 10.1016/j.margen.2016.06.005

Markou, G., Nerantzis, E. 2013. Microalgae for high-value compounds and biofuels production: a review with focus on cultivation under stress conditions. Biotechnol Adv. **31**, 1532–1542. https://doi.org/10.1016/j.biotechadv.2013.07.011

Martinez-Garcia, M., Kormpa, A., van der Maarel, M.J.E.C. 2017. The glycogen of Galdieria sulphuraria as alternative to starch for the production of slowly digestible and resistant glucose polymers. Carbohydr. Polym. **169**, 75–82. 10.1016/j.carbpol.2017.04.004

Martinez-Garcia, M., Stuart, M.C.A., van der Maarel, M.J.E.C. 2016. Characterization of the highly branched glycogen from the thermoacidophilic red microalga Galdieria sulphuraria and comparison with other glycogens. Int. J. Biol. Macromol. **89**, 12–18. 10.1016/j.ijbiomac.2016.04.051

Oesterhelt, C., Schmälzlin, E., Schmitt, J.M., Lokstein, H. 2007. Regulation of photosynthesis in the unicellular acidophilic red alga Galdieria sulphuraria. Plant J. **51**, 500–511. 10.1111/j.1365-313X.2007.03159.x

Paul, M.J., Pellny, T.K. 2003. Carbon metabolite feedback regulation of leaf photosynthesis and development. J. Exp. Bot. **54**, 539–547. 10.1093/jxb/erg052

Pinto, G., Albertano, P., Ciniglia, C., Cozzolino, S., Pollio, A., Yoon, H.S., Bhattacharya, D. 2003. Comparative approaches to the taxonomy of the genus Galdieria merola (Cyanidiales, Rhodophyta). CRYPTOGAMIE ALGOL. **24**, 13–32. https://eurekamag.com/research/010/350/010350883.php

Reeb, V., Bhattacharya, D. 2010. The thermo-acidophilic cyanidiophyceae (Cyanidiales). in: Seckbach, J., Chapman D.J., (Eds), Red algae in the genomic age, Springer, pp. 409–426. 10.1007/978-90-481-3795-4

Ritchie, R.J. 2006. Consistent sets of spectrophotometric chlorophyll equations for acetone, methanol and ethanol solvents. Photosynth Res. **89**, 27–41. 10.1007/s11120-006-9065-9

Rottet, S., Besagni, C., Kessler, F. 2015. The role of plastoglobules in thylakoid lipid remodeling during plant development. Biochim Biophys Acta. **1847**, 889–899. 10.1016/j.bbabio.2015.02.002

Sakurai, T., Aoki, M., Ju, X., Ueda, T., Nakamura, Y., Fujiwara, S., Umemura, T., Tsuzuki, M., Minoda, A. 2016. Profiling of lipid and glycogen accumulations under different growth conditions in the sulfothermophilic red alga Galdieria sulphuraria. Bioresour Technol. **200**, 861–866. 10.1016/j.biortech.2015.11.014

Schmidt, R.A., Wiebe, M.G., Eriksen, N.T. 2005. Heterotrophic high cell-density fed-batch cultures of the phycocyanin-producing red alga Galdieria sulphuraria. Biotechnol Bioeng. **90**, 77–84. 10.1002/bit.20417

Scott, S.A., Davey, M.P., Dennis, J.S., Horst, I., Howe, C.J., Lea-Smith, D.J., Smith, A.G. 2010. Biodiesel from algae: challenges and prospects. Curr Opin Biotechnol. **21**, 277–286. 10.1016/j.copbio.2010.03.005

Selvaratnam, T., Pegallapati, A., Montelya, F., Rodriguez, G., Nirmalakhandan, N., Lammers, P.J., Van Voorhies, W. 2015. Feasibility of algal systems for sustainable wastewater treatment. Renewable Energy. **82**, 71–76. https://doi.org/10.1016/j.renene.2014.07.061

Selvaratnam, T., Pegallapati, A.K., Montelya, F., Rodriguez, G., Nirmalakhandan, N., Van Voorhies, W., Lammers, P.J. 2014. Evaluation of a thermo-tolerant acidophilic alga, Galdieria sulphuraria, for nutrient removal from urban wastewaters. Bioresour Technol. **156**, 395–399. 10.1016/j.biortech.2014.01.075

Shimonaga, T., Konishi, M., Oyama, Y., Fujiwara, S., Satoh, A., Fujita, N., Colleoni, C., Buleon, A., Putaux, J.-L., Ball, S.G. 2008. Variation in storage α-glucans of the Porphyridiales (Rhodophyta). Plant Cell Physiol. **49**, 103–116. 10.1093/pcp/pcm172

Sloth, J.K., Jensen, H.C., Pleissner, D., Eriksen, N.T. 2017. Growth and phycocyanin synthesis in the heterotrophic microalga Galdieria sulphuraria on substrates made of food waste from restaurants and bakeries. Bioresour Technol. **238**, 296–305. 10.1016/j.biortech.2017.04.043

Sloth, J.K., Wiebe, M.G., Eriksen, N.T. 2006. Accumulation of phycocyanin in heterotrophic and mixotrophic cultures of the acidophilic red alga Galdieria sulphuraria. enzyme Microb Technol. **38**, 168–175. https://doi.org/10.1016/j.enzmictec.2005.05.010

Stadnichuk, I., Rakhimberdieva, M., Bolychevtseva, Y., Yurina, N., Karapetyan, N., Selyakh, I. 1998. Inhibition by glucose of chlorophyll a and phycocyanobilin biosynthesis in the unicellular red alga Galdieria partita at the stage of coproporphyrinogen III formation. Plant Sci. **136**, 11–23. https://doi.org/10.1016/S0168-9452(98)00088-0

Stadnichuk, I.N., Rakhimberdieva, M.G., Karapetyan, N.V., Bolychevtseva, Y.V., Boichenko, V.A., Selyakh, I.O. 2000. Glucose-induced inhibition of the photosynthetic pigment apparatus in heterotrophically-grown Galdieria partita. Russ. J. Plant Physiol. **47**, 585–592.

Takagi, M., Yoshida, T. 2006. Effect of salt concentration on intracellular accumulation of lipids and triacylglyceride in marine microalgae Dunaliella cells. J. Biosci. Bioeng. **101**, 223–226. 10.1263/jbb.101.223

Tischendorf, G., Oesterhelt, C., Hoffmann, S., Girnus, J., Schnarrenberger, C., Gross*, W. 2007. Ultrastructure and enzyme complement of proplastids from heterotrophically grown cells of the red alga Galdieria sulphuraria. Eur J Phycol. **42**, 243–251. https://doi.org/10.1080/09670260701437642

Toplin, J.A., Norris, T.B., Lehr, C.R., McDermott, T.R., Castenholz, R.W. 2008. Biogeographic and phylogenetic diversity of thermoacidophilic cyanidiales in Yellowstone National Park, Japan, and New Zealand. Appl Environ Microbiol. **74**, 2822–2833. 10.1128/AEM.02741-07

Van Wychen, S., Laurens, L. 2013. Determination of Total Lipids as Fatty Acid Methyl Esters (FAME) by in situ Transesterification: Laboratory Analytical Procedure (LAP). National Renewable Energy Laboratory (NREL), Golden, CO. 10.2172/1118085

Viola, R., Nyvall, P., Pedersén, M. 2001. The unique features of starch metabolism in red algae. Proc R Soc Lond B Biol Sci. Series B*:* Biological Sciences. **268**, 1417–1422. https://doi.org/10.1098/rspb.2001.1644

Vítová, M., Bišová, K., Umysová, D., Hlavová, M., Kawano, S., Zachleder, V., Čížková, M. 2011. Chlamydomonas reinhardtii: duration of its cell cycle and phases at growth rates affected by light intensity. Planta. **233**, 75–86. 10.1007/s00425-010-1282-y

Wan, M., Liu, P., Xia, J., Rosenberg, J.N., Oyler, G.A., Betenbaugh, M.J., Nie, Z., Qiu, G. 2011. The effect of mixotrophy on microalgal growth, lipid content, and expression levels of three pathway genes in Chlorella sorokiniana. Appl Microbiol Biotechnol. **91**, 835–844. 10.1007/s00253-011-3399-8

Wang, H., Xiong, H., Hui, Z., Zeng, X. 2012. Mixotrophic cultivation of Chlorella pyrenoidosa with diluted primary piggery wastewater to produce lipids. Bioresour Technol. **104**, 215–220. 10.1016/j.biortech.2011.11.020

Widdel, F. 2007. Theory and measurement of bacterial growth. In: Grundpraktikum Mikrobiologie, University of Bremen, Germany. **4**, 1–11.

Zhang, L., Happe, T., Melis, A. 2002. Biochemical and morphological characterization of sulfur-deprived and H 2-producing Chlamydomonas reinhardtii (green alga). Planta. **214**, 552–561. https://doi.org/10.1007/s004250100660

Figure Captions

Figure 1. Growth curve and nutrient determination. **A.** Culture growth in *G. sulphuraria* under autotrophic (A) mixotrophic (M) and heterotrophic (H) conditions. **B**. Ammonium uptake and **C**. Phosphate quantification from the supernatant. The supernatant was collected daily and analyzed for the ammonium and phosphate uptake in a microplate assay. The initial concentration of ammonium was 350 ppm and the phosphate concentration was188 ppm. Error bars indicate SE (n=3).

Figure 2. Biomass yield and substrate uptake. **A.** Biomass yield in both growth conditions H (heterotrophy) and M (mixotrophy). **B.** Corn stover saccharide uptake rate in heterotrophic and **C.** mixotrophic cultures. Error bars indicate SE (n=3).

Figure 3. Photosynthetic measurements. **A.** O_2 evolution of autotrophic (A) mixotrophic (M) and heterotrophic (H) cultures in *G. sulphuraria*. **B**. Micrograms of Chlorophyll *a* per culture volume of A, M and H cultures. **C.** O_2 evolution per mg of chlorophyll per min (values were normalized to mg of chlorophyll). **D.** Phycocyanin production (mg g^{-1} AFDW) under A, M and H growth conditions. Cells were harvested in the exponential (Day4) (E), and stationary phases (Day7) (S). Letters represent the statistical significance between the treatments. Error bars indicate SE (n=3).

Figure 4. Electron micrographs of ultrastructure of *G. sulphuraria*. The cells are in the **A.** Exponential phase and **B.** Stationary phase of autotrophic, **C.** Exponential and **D.** Stationary phase of mixotrophic, **E.** Exponential and **F.** Stationary phase of heterotrophic culture conditions. Labels: CP – Chloroplast; N – Nucleus; LB – Lipid Bodies; FS – Floridean Starch; CW – Cell Wall.

Figure 5. Biochemical analysis of carbon allocation. **A.** Accumulation of starch and **B.** β-glucan in *G. sulphuraria***. C.** Total fatty acid content from autotrophic (A), mixotrophic (M) and heterotrophic (H) cultures. **D.** Fatty acid profiles of photoautotrophic, **E**. mixotrophic and **F**. heterotrophic conditions. Cells were harvested in the exponential (E), stationary (S) phases and quantified per dry weight. Letters represent the statistical significance between the treatments. Error bars indicate SE (n=3)."

Graphical Abstract

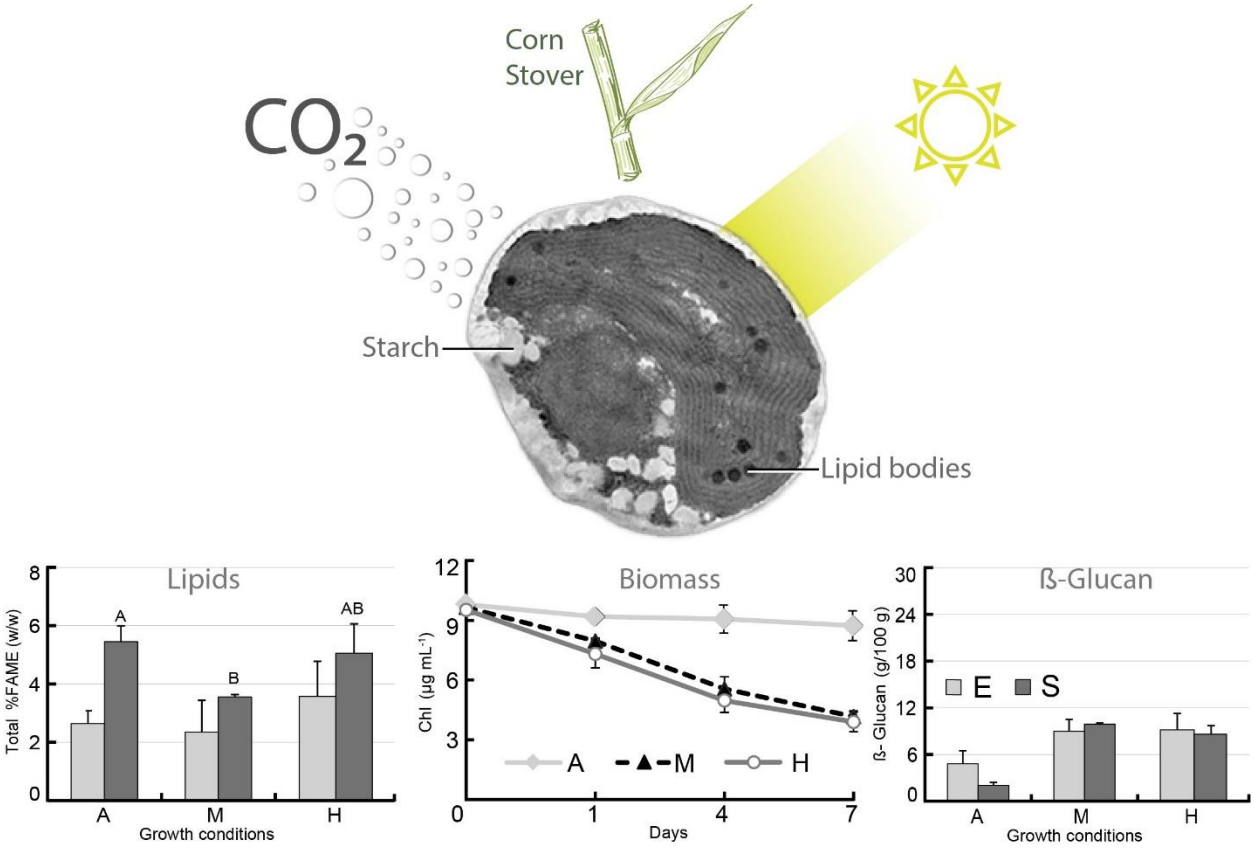

Figure 1

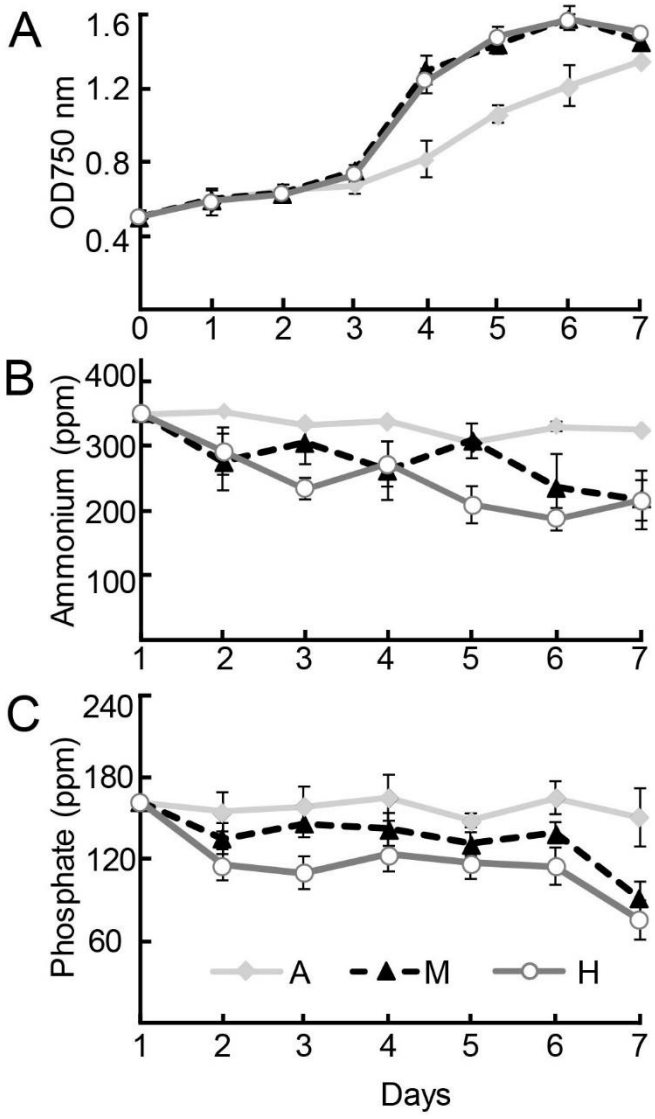
A
OD750 nm
1.6
1.2
0.8
0.4
0
1
2
3
4
5
6
7
B
Ammonium (ppm)
400
300
200
100
1
2
3
4
5
6
7
C
Phosphate (ppm)
240
180
120
60
A
M
H
1
2
3
4
5
6
7
Days

Fig 2

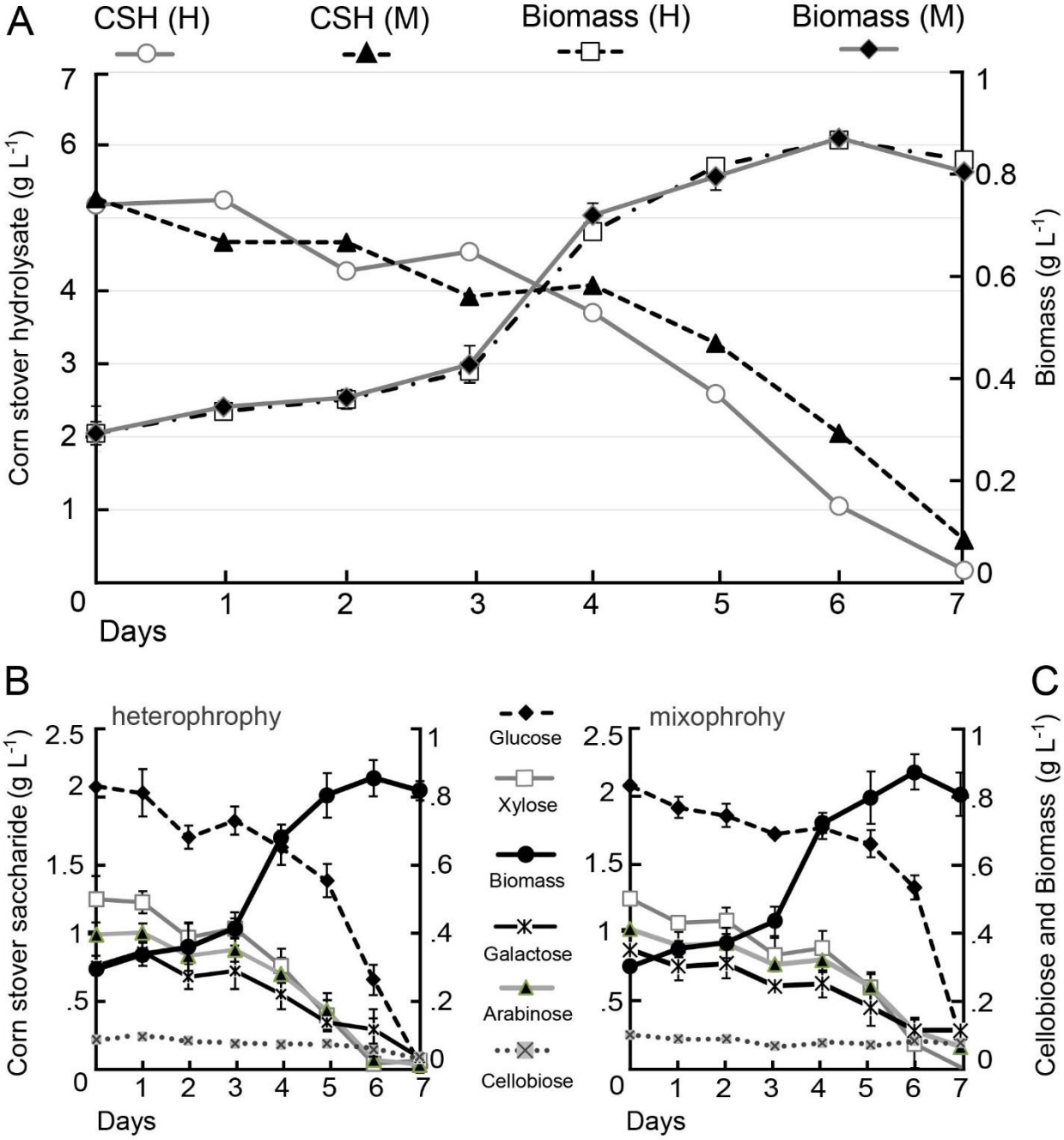
A
CSH (H)
CSH (M)
Biomass (H)
Biomass (M)
Corn stover hydrolysate (g L-1)
Biomass (g L-1)
Days
B
heterophrophy
Corn stover saccharide (g L-1)
Days
Glucose
Xylose
Biomass
Galactose
Arabinose
Cellobiose
C
mixophrohy
Cellobiose and Biomass (g L-1)
Days

Figure 3

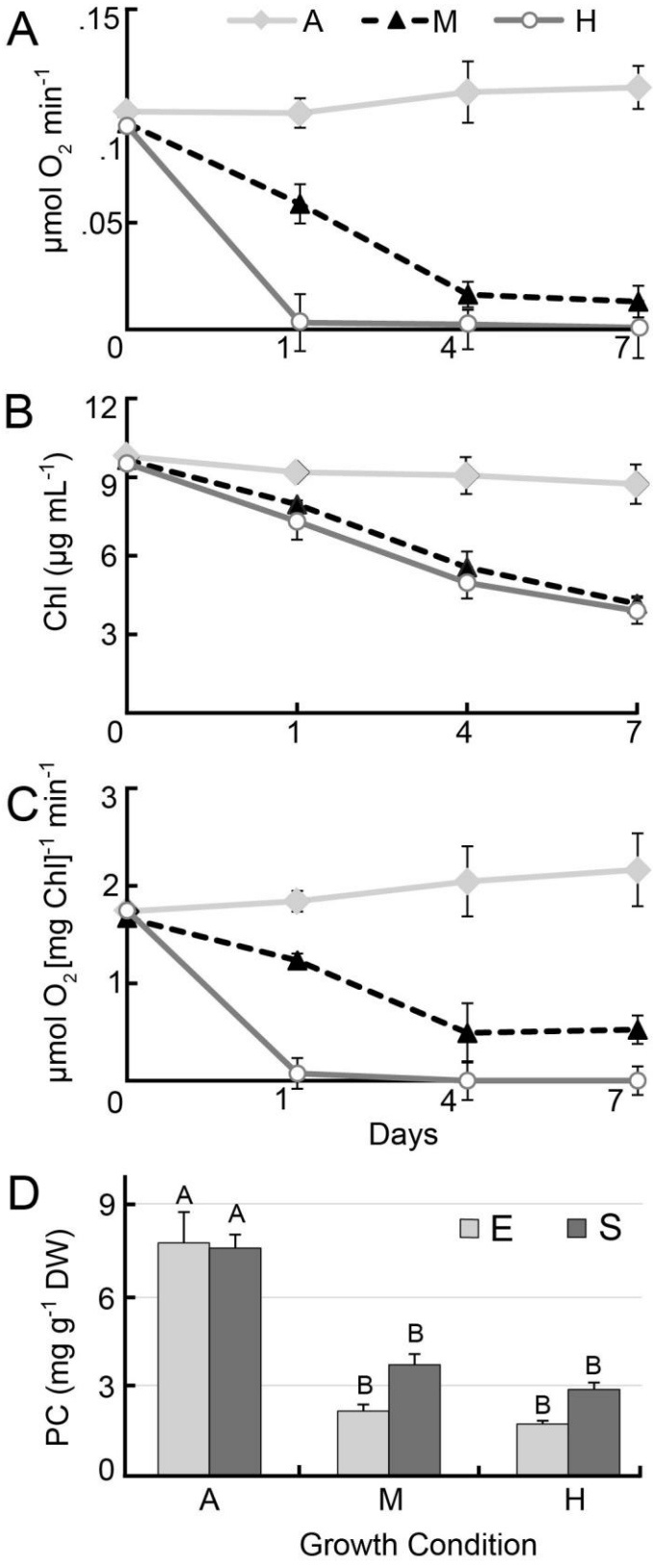
A
.15
.1
.05
0
1
4
7
A
M
H
µmol O2 min-1
B
12
9
6
3
Chl (µg mL-1)
C
3
2
1
µmol O2 [mg Chl]-1 min-1
Days
D
9
6
3
PC (mg g-1 DW)
E
S
A
M
H
Growth Condition

Figure 4

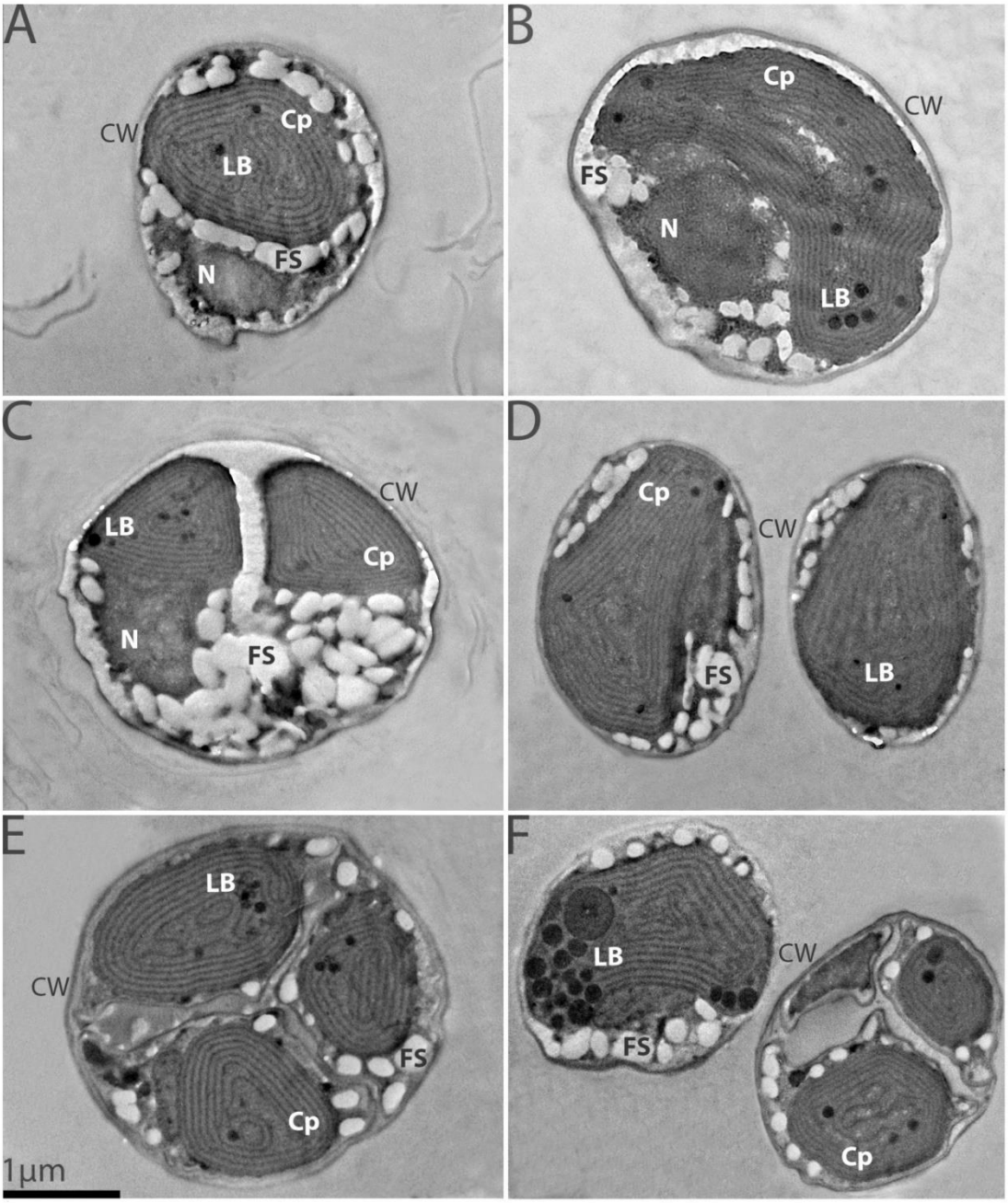
A
CW
Cp
LB
FS
N
B
Cp
CW
FS
N
LB
C
CW
LB
Cp
N
FS
D
Cp
CW
FS
LB
E
LB
CW
FS
Cp
1µm
F
LB
CW
FS
Cp

Figure 5

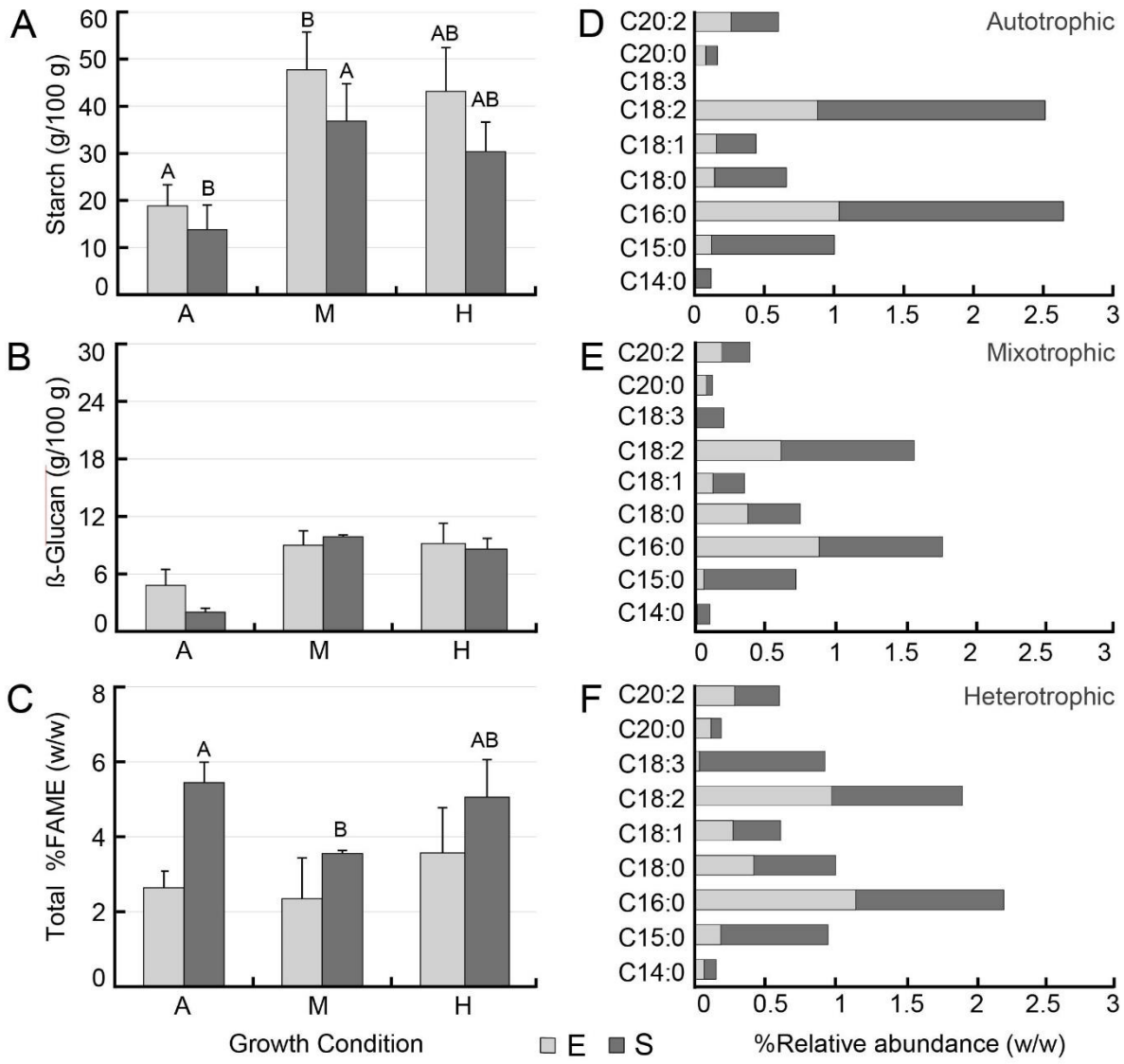
A
Starch (g/100 g)
60
50
40
30
20
10
0
A
B
B
A
AB
AB
A
M
H
B
ß-Glucan (g/100 g)
30
24
18
12
6
0
A
M
H
C
Total %FAME (w/w)
8
6
4
2
0
A
B
AB
A
M
H
Growth Condition
E
S
D
Autotrophic
C20:2
C20:0
C18:3
C18:2
C18:1
C18:0
C16:0
C15:0
C14:0
0
0.5
1
1.5
2
2.5
3
E
Mixotrophic
C20:2
C20:0
C18:3
C18:2
C18:1
C18:0
C16:0
C15:0
C14:0
0
0.5
1
1.5
2
2.5
3
F
Heterotrophic
C20:2
C20:0
C18:3
C18:2
C18:1
C18:0
C16:0
C15:0
C14:0
0
0.5
1
1.5
2
2.5
3
%Relative abundance (w/w)

Supplemental Figures

Figure S1

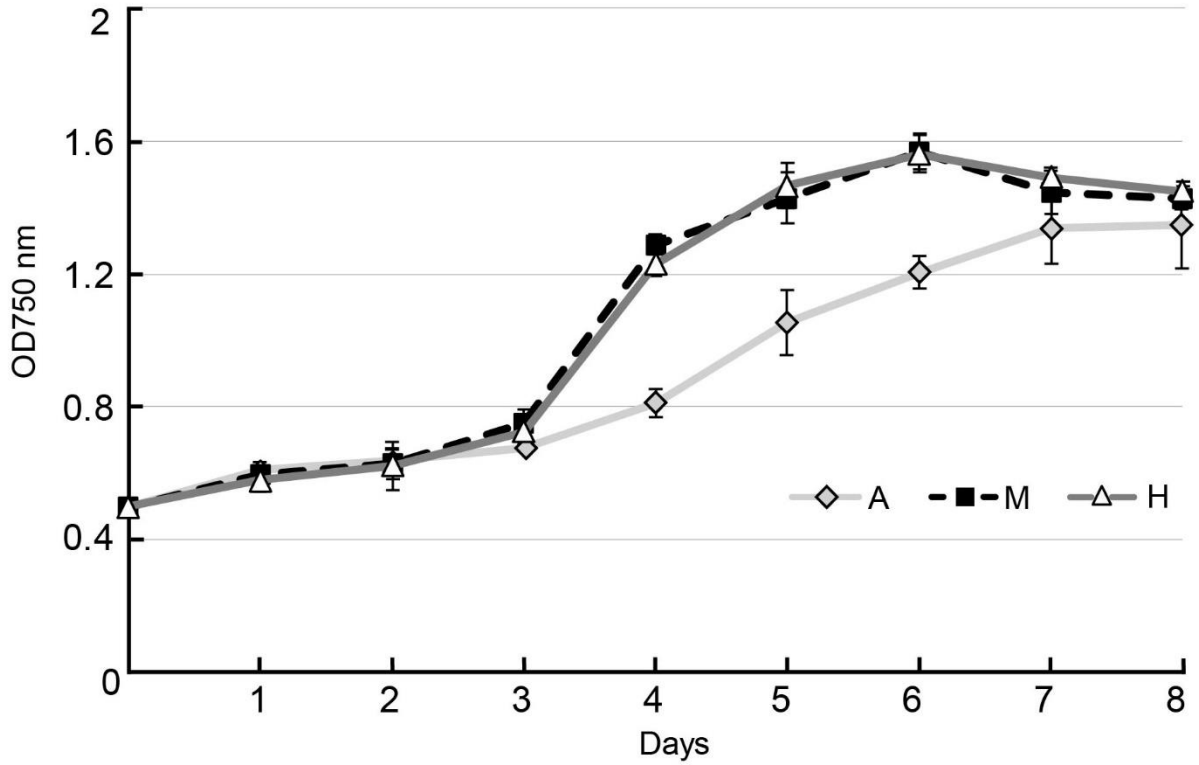

Figure S2